JOURNAL OF MATERIALS RESEARCH AND TECHNOLOGY 2023;23:2371–2388

Available online at www.sciencedirect.com

jmr&t Journal of Materials Research and Technology

journal homepage: www.elsevier.com/locate/jmrt

Original Article

Experimental investigation of a sustainable reinforced cantilever concrete slab exposed to different intensity of temperatures

Diyar N. Qader [a], M.K. Haridharan [b], G. Murali [c], Sallal R. Abid [d], Parthiban Kathirvel [e], Amran Mugahed [f,g,*], Roman Fediuk [c,h], Ali M. Onaizi [i]

[a] Department of Civil Engineering, Cihan University-Erbil, Erbil 44001, Kurdistan Region, Iraq
[b] National Institute of Technology, Arunachal Pradesh, 791113, Arunachal Pradesh, India
[c] Division of Research & Innovation, Uttaranchal University, Dehradun 248 007, India
[d] Department of Civil Engineering, Wasit University, Kut 52003, Iraq
[e] School of Civil Engineering, SASTRA Deemed University, Thanjavur 613401, India
[f] Department of Civil Engineering, College of Engineering, Prince Sattam Bin Abdulaziz University, 11942 Alkharj, Saudi Arabia
[g] Department of Civil Engineering, Faculty of Engineering and IT, Amran University, 9677, Amran, Yemen
[h] Polytechnic Institute, Far Eastern Federal University, 690922 Vladivostok, Russia
[i] School of Architecture and Built Environment, University of Newcastle, Callaghan, NSW, 2308, Australia

ARTICLE INFO

Article history:
Received 17 November 2022
Accepted 24 January 2023
Available online 31 January 2023

Keywords:
Stiffness
Elevated temperature
Cooling regimes
Cantilever slab
Cracks

ABSTRACT

Recently, several scientists have paid special attention to how high temperatures alter the chemical and physical features of reinforced concrete structural members such as slabs. Cantilever concrete slabs, the impact of cooling regimes, the influence of the crack created during heating, and the residual strength of concrete slabs subjected to extreme temperatures were very limitedly investigated in the reviewed literature. Therefore, this research investigated the behavior of cantilever concrete slabs subjected to elevated temperatures and cooling regimes. Two different slab thicknesses (100 mm and 150 mm), various intensity of temperature (200 °C, 300 °C, 400 °C and 500 °C) and two different cooling conditions (Air and Quench cooling) were examined. The observations made during the thermal loadings were the moisture movement, deformation, crack patterns, and temperature on the slab's exposed (bottom) and unexposed surface (top). The results indicated that the magnitude of temperature influences all the tested specimens. In the quench-cooled condition, the development of cracks was increased in the non-exposed slab surface when heated at 300 °C, 400 °C and 500 °C. The severity of the exposed temperature and cooling regimes also affected the concrete slab's irreversible loss of flexural stiffness. The flexural stiffness reduction of the 100 mm thick slab varied from 1.68% to 35.52% for a temperature range of 200 °C–500 °C under air-cooled conditions, while for the quench-cooled specimens, the stiffness reduction varied between 0.88% and 45.92% for the same temperature range. On the other hand, increasing the slab thickness from 100 to 150 mm

* Corresponding author. Department of Civil Engineering, College of Engineering, Prince Sattam Bin Abdulaziz University, 11942 Alkharj, Saudi Arabia
E-mail address: m.amran@psau.edu.sa (A. Mugahed).
https://doi.org/10.1016/j.jmrt.2023.01.180

decreased the stiffness reduction, where the stiffness reduced by 1.02%–24.61% and 0.28% –32.17% for the cases of air and water coolings, respectively.

1. Introduction

In recent years, scientists have paid special attention to how high temperatures alter the chemical and physical features of reinforced concrete (RC) buildings [1,2]. Research done between 1980 and 2012 found that out of 40 bridges that collapsed, only 20 were attributable to seismic loads, suggesting that fire was the primary cause of the collapse. This result highlights the need to study the impact of fire on RC structures, particularly RC slabs [3]. Fire behavior in RC constructions can be affected by several factors, including porosity, moisture content, boundary conditions, concrete cover, reinforcing bars, geometrical properties and concrete's thermal and mechanical properties [4–7]. In the event of a fire, buildings and flooring will suffer damage [8,9]. Recent studies have used experimental and numerical techniques to examine the fire behavior of reinforced concrete slabs, including reinforced continuous concrete or prestressed slabs [10,11], in-plane restrained slabs [12,13] and simply supported slabs [14,15]. The thirst for understanding the behavior of a structure subjected to elevated temperature increased after the collapse of the World Trade Center, the fire damage observed in the Windsor Tower building and the Architecture building at Delft University. Several researchers have performed on RCC structural elements to investigate the load carrying capacity of a structure subjected to fire [16–20]. One-way concrete slabs were tested for their structural integrity after being exposed to three different types of fires (a fire either underneath or above the slab, or both) by Shachar and Dancygier [21]. These findings suggest that it is important to evaluate not only the reduced ductility of a structure after a fire but also its load-bearing capacity.

Wang et al. [22] tested four continuous RC slabs while subjecting them to varying compartment fires. The failure mechanism of the RC slabs had an impact on the reinforcing pattern and ratio. Additionally, Wang et al. [23,24] studied the post-fire behavior of continuous RC slabs exposed to various fire conditions. It has been demonstrated that situations involving compartment fires and concrete's mechanical characteristics impact the failure mechanism and the ultimate load-bearing capacity. Yu [25] studied the mechanical performance of continuous slabs (four two-span one-way) of size 5200 × 1200 × 120 mm) exposed to fire. Tests conducted on fire-damaged continuous slabs revealed that the fire's duration had a greater impact on their initial stiffness than the residual limit capacity. Nevertheless, because to different boundary conditions, the findings from the one-way slabs can't be extrapolated to the two-way ones. Fabricio et al. [26] carried out a series of fire experiments on a total of eight concrete slabs measuring 2.56 × 4.60 m and decking made of composite steel. As a consequence of this, the composite behavior of the slab (structural integrity, membrane effect) persisted for roughly 5 min (10 min, a time that ranged between 30 and 50 min) of exposure to fire. The research showed that the top bars did not effectively keep the slab together.

Several researchers reported the failure modes of RCC slabs mainly by fracturing or yielding reinforcement and crushing concrete [21,27]. Few researchers developed analytical methods to predict ultimate load using advanced computational capabilities by considering various failure criteria [28,29]. The tests were performed for standard fire conditions, under service level of loading, for one way and two slabs. In two-way slabs additional load-carrying capacity was due to the formation of double curvature membrane action [30]. Zhang and Dong [31] developed a new analytical technique for determining the concrete slabs load-carrying capacity limits when exposed to fire. The limit load was calculated using a traditional segmented equilibrium approach. Upon creating the plastic hinge mechanism, it was discovered that the tensile membrane action contributed to the vertical reinforcement's tensile force. The plastic hinge line pattern's response to the end moment of constraint might be predicted using this mathematical model [32]. Research by Guo and Bailey [33] was done on composite slabs under various fire scenarios, considering both the fires' heating and cooling phases. The heating rate determined the behavior of composite slabs, the highest temperature achieved, the duration the slabs were exposed to fire, and the rate at which they cooled. The fire scenario with maximum temperature resulted in maximum deflection in a fire scenario with lower temperatures. However, the increased duration of exposure caused the maximum temperature on the unexposed surfaces during the cooling stages. The maximum temperature on an unexposed side was reached during the increased cooling rate [6,34]. The fire's cooling process had a significant impact on structural behavior.

Huang [35] created a reliable model for thoroughly studying a uniformly loaded reinforced concrete slab subject to varying degrees of concrete spalling under a conventional fire regime. A total of 16 examples were investigated, each of which used a unique degree of spalling on slabs and included varying localized fire chambers in terms of their magnitude and location [35]. The fire compartment's floor slabs are clearly protected from excessive heat buildup thanks to the presence of nearby cold buildings. It is clear that the compressive membrane force inside the slabs is a significant factor in lowering the influence that concrete spalling has on the structural behavior of floor slabs when they are exposed to fire. After being exposed to fire for 60 or 120 min, thermocouples inserted in the slab thickness recorded temperature changes ranging from 250–600 °C to 450–900 °C, respectively, according to study by Colombo et al. [36]. Al-Ameri et al. [37] reported that the engineered cementitious composites heated to temperatures of 100 and 200 °C did not significantly alter their impact resistance, resulting in greater or slightly lower

impact resistance compared to the unheated specimens. The impact resistance and ductility of the material significantly decreased when heated to 300 °C. The fire safety implications of computational modeling for reinforced concrete structures were examined in detail by Ni et al. [34]. In addition, the effects of cooling phases after actual thermal exposures on material characteristics and deformations, the unpredictability of the reactions of materials and structures when subjected to high temperatures, and model response as a function of tensile fracture energy. Possible failure modes during and after the cooling phase of a fire should be modeled numerically, and it is recommended that such models be developed for RC buildings. This could happen because of slow heat transfer rate between the portions and intricate stress redistributions.

Limited published data available on axial elongation and the effect of thermal curvature due to non-linear thermal gradient across the thickness of slab resulted in enhancement of the vertical deflection of the slab [38]. In general, a floor system has to satisfy multiple functions like (a) load-bearing (R) (b) integrity (E) (c) insulation (I) and (d) impact resistance (M). In most cases, integrity, insulation and temperature in reinforcement are limiting criteria to assess the failure of slabs under standard fire circumstances. Earlier studies focused on simply supported and continuous slab systems subjected to standard fire conditions. Cantilever concrete slabs, the impact of cooling regimes, the influence of the crack created during heating, and the residual strength of concrete slabs subjected to extreme temperatures were all found to be lacking in experimental data in the literature review. The concrete compressive strength and stiffness were negatively impacted by cooling regimes such as air and quench cooling conditions. The studies on concrete under elevated temperatures by various authors [39–44] suggested that the compressive strength of the concrete decreases drastically when the specimens are exposed to a temperature of 600 °C and higher temperatures. However, it also depends on the temperature intensity and exposure duration [39]. Thus, when a structural concrete element reaches such high temperatures, the strength drops significantly so that the residual strength becomes lower than the minimum structural concrete requirements, which makes the repairing decision unsuitable. As the focus of this study is on the residual strength of the beams, the specimens were subjected to the temperature range of 200 °C–500 °C with an increment of every 100 °C. The residual strength of concrete specimens cooled with water for a short time exhibited a dramatic fluctuation when the temperature was more than 200 °C [40,41].

This study evaluates the post-fire behavior of cantilever RC slabs after exposure to various high temperatures and cooling regimes to asses the residual strength. First, the furnace temperatures in addition to concrete and steel temperatures of the slabs and serviceability conditions were briefly investigated. Second, the residual strength of fire-damaged slabs and three reference slab were loaded to failure at ambient temperature. The vertical and horizontal deflections, cracking patterns, and failure modes were investigated for each slab. However, the need is to assess the level of damage based on the specimen's load-bearing capacity and flexural stiffness [13,22]. Therefore, the research focuses on the temperature at the non-exposed surface, crack formation, and crack width during the heating and cooling stages, during the mechanical loading stage mode at failure, the behavior of the cantilever slab, and the variation in residual strength and flexural stiffness. Finally, the residual ultimate limit loads and flexural stiffness predicted in this experimental study are presented. The results obtained from this study are useful in assessing canopy structures subjected to elevated temperatures and provide valuable engineering conclusions.

2. Experimental research

2.1. Methodology

The present study investigates the impact of the cooling phase on residual strength and stiffness at the material level, focusing on the behavior of reinforced concrete slabs subjected to elevated temperatures. The element level testing is essential to quantify the residual strength of the elements. This quantification will help the stakeholders determine whether the elements require strengthening or demolishing and whether reconstruction is the only solution. The entire study was conducted in two phases, a) Thermal Loading and b) Mechanical Loading on the slab. In the first phase, the slab elements with 100 mm and 150 mm thickness were subjected to temperatures of 200 °C, 300 °C, 400 °C and 500 °C for a retention period of 4 h at that specific temperature. The temperature loading on the specimens were applied through the electric furnace. After exposure to the desired temperature and duration, the specimen was subjected to two types of cooling regimes (Air-cooled and Quench Cooled). In the second phase, the study further focused on the evaluation of residual behavior and stiffness degradation under two different cooling conditions by conducting load test on the slab elements.

2.2. Materials

The M25 concrete grade with mix ratio of 1: 1.85: 3.12 with water cement ratio of 0.5 was considered for this study. The concrete mix proportions are arrived based on the IS: 10,262–2009 [45] standard and the same mix proportions used in our earlier study [46]. The ordinary Portland cement of 43 grade was used as binding agent conforming to BIS-8112 [47] and Class F fly ash (Neyveli Lignite Corporation) in accordane with ASTM C 618 [48] and BIS-3812 [49]. The cement used for the study was proportioned in a ratio of 70:30 where 70% was Ordinary Portland Cement (OPC) and 30% was fly ash. The fine aggregate used had a fineness modulus of 2.44, specific gravity of 2.65 and was in confirmation with Zone – II grading. Two sizes of coarse aggregate used were 20 mm and 12.5 mm, in a mix proportion of 50% each. The combined fineness modulus was 6.55 and specific gravity 2.75.

2.3. Details of slab

The concrete slab thickness provided in India's dwelling units and commercial buildings ranges from 100 mm to 150 mm. The slab thickness and reinforcements used in this research are the same as the actual structure. The geometry and

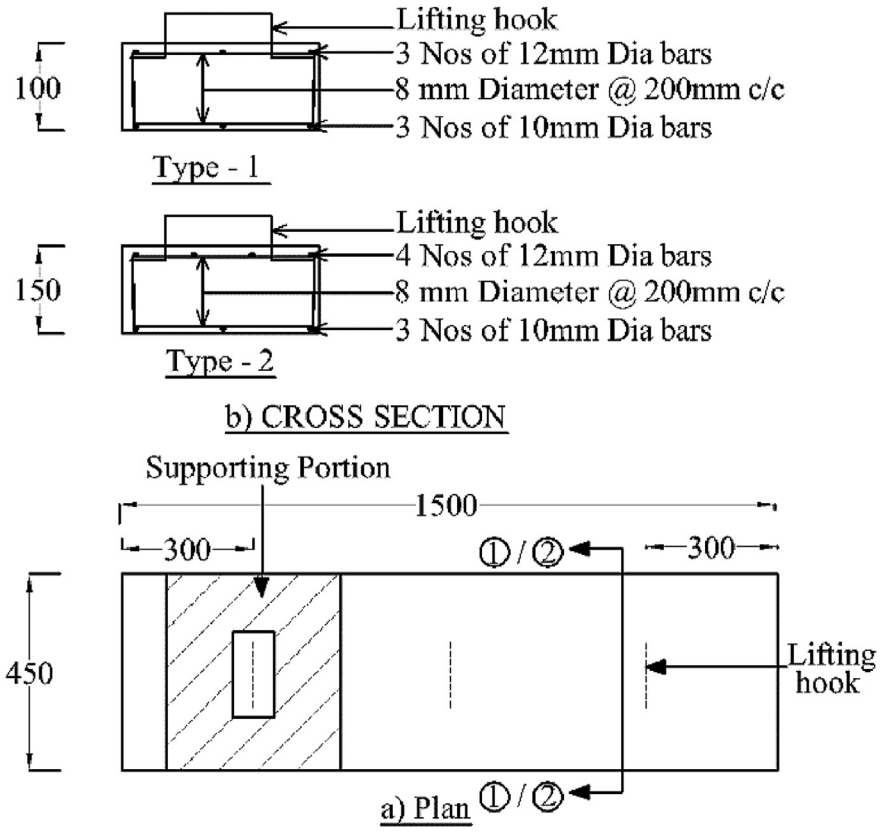

Fig. 1 – Schematic sketch of reinforced concrete slab is shown in a) Plan view and b) Cross section details.

reinforcement details of the slab elements were fixed, as shown in Fig. 1. The slab dimensions considered in the study represented the canopy/cantilever projection provided in the dwelling and commercial buildings to facilitate the stakeholder's requirement. The slab dimension was 450 mm in width, 1500 mm in length and the distance between the support and free end was 1000 mm. The roof slab thickness in most existing structures varies from 100 mm to 150 mm, while the present study focused on 100 mm and 150 mm thickness. All slabs were fabricated in 8 days and 6 specimens per day.

In this research, 48 numbers of specimens were prepared, having plan dimensions of 450 mm × 1500 mm which were constant for all the specimens. The study aimed to investigate the effects of (i) Thickness of slab (100 mm and 150 mm), (ii) magnitude of temperature (200 °C, 300 °C, 400 °C and 500 °C) and (iii) Cooling Regimes ((Air cooled (AC or D) and Quench cooling (QC or Q) "Water is sprayed for 30 min at the exposed surface of the slab"). The notations used to describe the slabs for the experiments are provided in Table 1. The compressive strength was found from 27 cubic specimens, which were cast along with each batch of slab casting. The spread of concrete grade considered in the study was evaluated using the compressive strength of concrete, the standard deviation was 0.70. The low value of standard deviation confirms the consistency of concrete grade. The average strength of concrete cube was 26.78 MPa with coefficient of variance was 0.03. The reinforcement rod of diameter 12 mm and 8 mm was used and its average tensile strength was 565.9 and 573.3 MPa respectively.

2.4. *Electrical furnace*

A mobile electrical furnace was fabricated in-house to facilitate the experimental study. The heating capacity of the furnace was 700 °C. The accuracy of the furnace was ±10 °C. The outer dimension of the furnace was 700 mm × 1500 mm. The furnace was layered with refractory bricks and encased with insulated steel plates at the sides and the bottom of the furnace. The opening at the top of the furnace was 450 mm × 1250 mm. The control box consists of an electrical circuit with a relay to connect to an external power source and a digital indicator to display the furnace temperature. Thermocouples are placed inside the furnace at a height of 300 mm from the heating coil to sense the temperature and provide a signal to the relay, which automatically trips down or starts again to maintain the desired temperature inside the furnace. Fig. 2 depicts the slab heating setup and furnace's time-temperature curves.

2.5. *Instrumentation and test procedure*

The experiments were performed in two phases; in the first phase, a slab was subjected to thermal loading at the desired temperature and for a preferred duration under its self-weight. In the second phase, load testing was conducted on heated and cooled specimens. Fig. 3 demonstrates the location and various monitoring devices used for thermal loading. Three thermocouple trees are placed at 550 mm from the free end to measure the temperature variation across the depth of

Table 1 – Mixture ID, and reinforcement details of the concrete slab.

No.	Mixture ID	Description	Reinforcement Details
1	NRT - 100	100 mm thick slab not exposed to temperature.	Main Reinforcement - Top – 3 nos of 12 mm diameter.
2	S1-D-100	100 mm thick slab subjected to 200 °C and air cooled	Bottom – 3 Nos of 10 mm diameter.
3	S1-Q-100	100 mm thick slab subjected to 200 °C and quench cooled.	Distributor – 8 mm diameter @ 150 mm c/c
4	S2-D-100	100 mm thick slab subjected to 300 °C and air cooled	
5	S2-Q-100	100 mm thick slab subjected to 300 °C and quench cooled.	
6	S3-D-100	100 mm thick slab subjected to 400 °C and air cooled	
7	S3-Q-100	100 mm thick slab subjected to 400 °C and quench cooled.	
8	S4-D-100	100 mm thick slab subjected to 500 °C and air cooled	
9	S4-Q-100	100 mm thick slab subjected to 500 °C and quench cooled.	
10	NRT - 150	150 mm thick slab not exposed to any temperature	Main Reinforcement - Top – 4 nos of 12 mm diameter.
11	S1-D-150	150 mm thick slab subjected to 200 °C and air cooled	Bottom – 3 Nos of 10 mm diameter.
12	S1-Q-150	150 mm thick slab subjected to 200 °C and quench cooled.	Distributor – 8 mm diameter @ 150 mm c/c
13	S2-D-150	150 mm thick slab subjected to 300 °C and air cooled	
14	S2-Q-150	150 mm thick slab subjected to 300 °C and quench cooled.	
15	S3-D-150	150 mm thick slab subjected to 400 °C and air cooled	
16	S3-Q-150	150 mm thick slab subjected to 400 °C and quench cooled.	
17	S4-D-150	150 mm thick slab subjected to 500 °C and air cooled	
18	S4-Q-150	150 mm thick slab subjected to 500 °C and quench cooled	

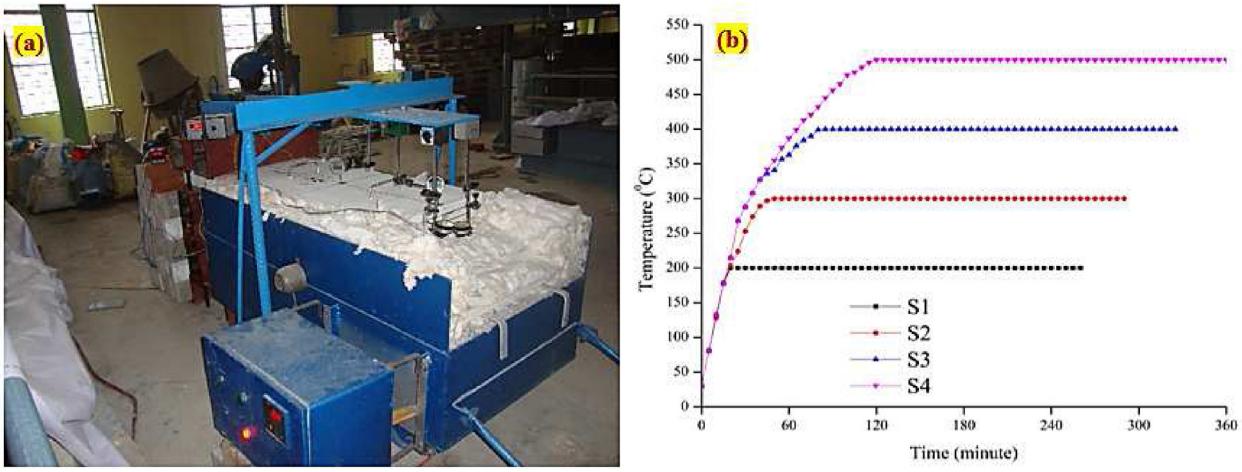

Fig. 2 – (a) Slab heating setup (b) Time – Temperature curve of furnace.

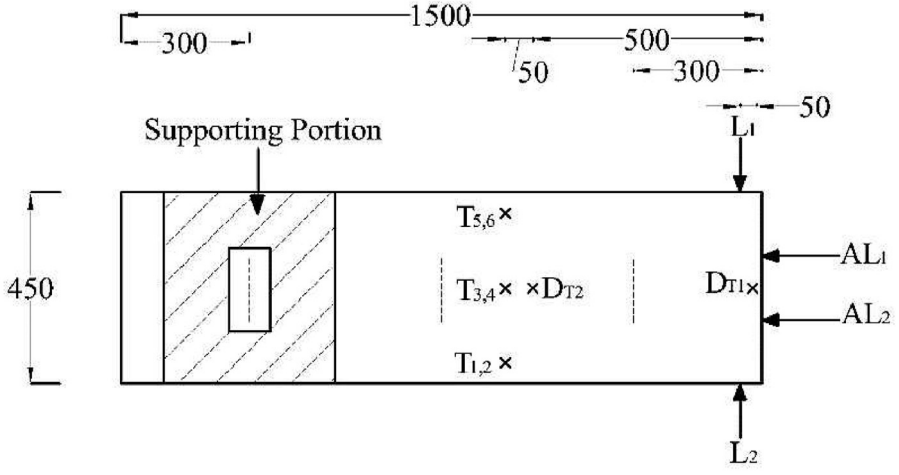

$T_{1,3,5}$–Thermocouple-Temperature measurement-at bottom of slab

$T_{2,4,6}$–Thermocouple-Temperature measurement-at top of slab

$L_{1,2}$, $AL_{1,2}$, $D_{T1,2}$ – Dial Gauge-Deformation measurement

Fig. 3 – Schematic sketch shows the instrumentation and its location considered during thermal loading.

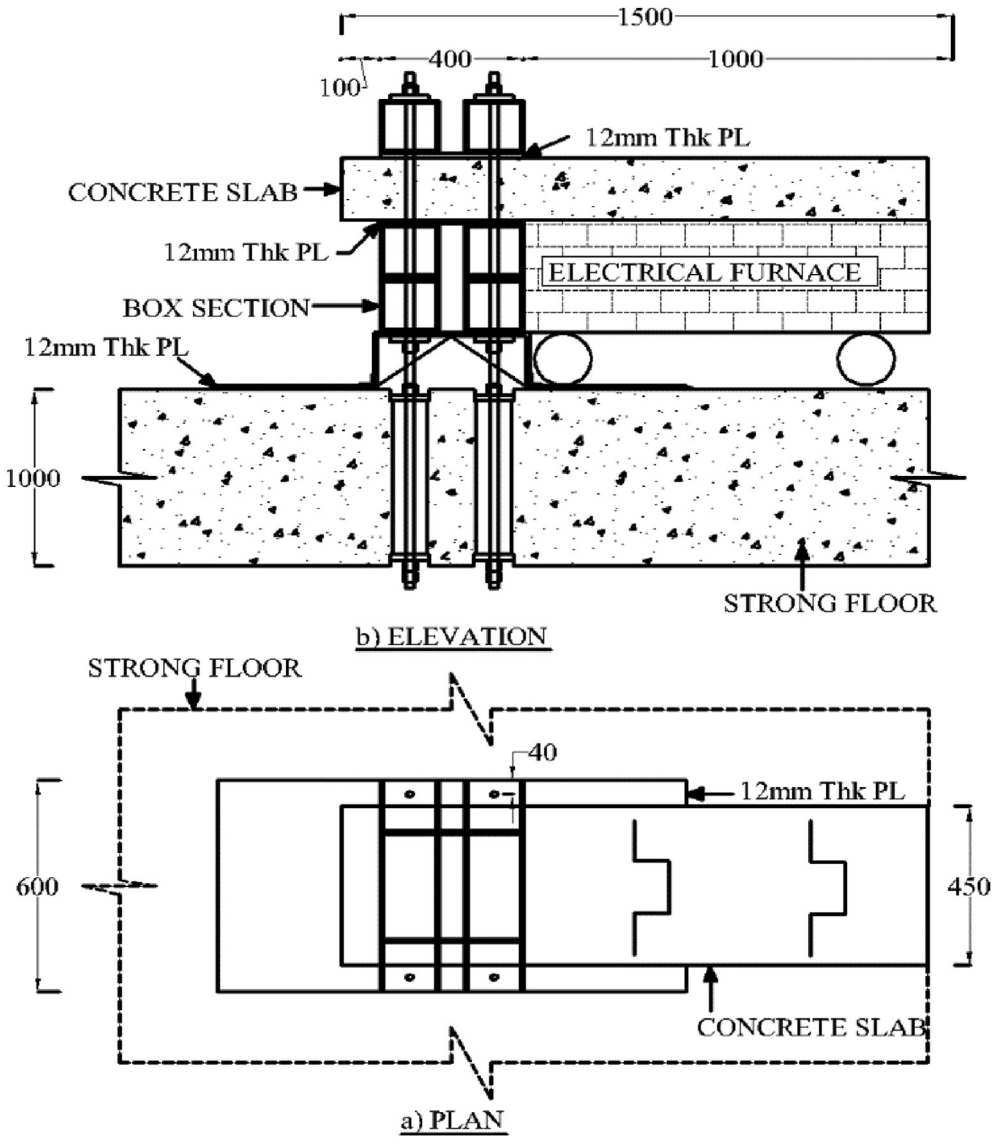

Fig. 4 – Schematic sketch of the experimental setup for thermal loading.

the section and; one tree is placed at the center and another two are 50 mm from the sides. These thermocouple trees provide the temperature variation from in-plan dimensions. The linear variable differential transducers (LVDT) are provided in all three directions to measure the elongations that occurred during the heating face of the experiment. Two numbers of LVDT's are provided along the length to measure the deflection at the free end and mid-span. Similarly, to measure the axial elongation, two LVDTS AL1 and AL2 are provided along the thickness of the slab at the free end. The schematic sketch and picture of the experimental setup are shown in Fig. 4. The thermal boundary condition of the concrete slab was that the bottom of the slab was subjected to heat flux from the electric furnace, and all sides were subjected to convection with air. The temperatures at the top and bottom surfaces of the slab were measured using thermocouples trees and dial gauges to measure the slab's deformation. The side surface of the slab was coated in pink colour to differentiate the colour change along with the depth of the slab. A quench or air cooling was used to cool the specimens after the slab was heated to the correct temperature and time. In the case of the air-cooled condition, the heated slabs were exposed to the atmosphere until the slab loading test in the next day. Thus, the slabs were left to be air cooled for approximately 12 h. Whereas for a quench-cooled slab, water was sprayed on the heated surface of the slab immediately after heating. The water was sprayed for 30 min and then left open to the atmosphere. The water used for spraying was maintained at room temperature (27 °C ± 5 °C).

The experimental setup and details of instrumentation used for the second phase are shown in Fig. 5. Three numbers of LVDT were placed along the length of a slab at 20 mm from the free end, 500 mm from the free end and 700 mm to the free end. The LVDT's are used to measure the vertical displacement of the element along the length. It provides an understanding of the deflected profile and provides an idea of damages that occurred either at the material level or at the geometry level. The load was applied as line load at the free end of the cantilever slab using a 200 metric ton power-controlled hydraulic jack. The applied load was measured

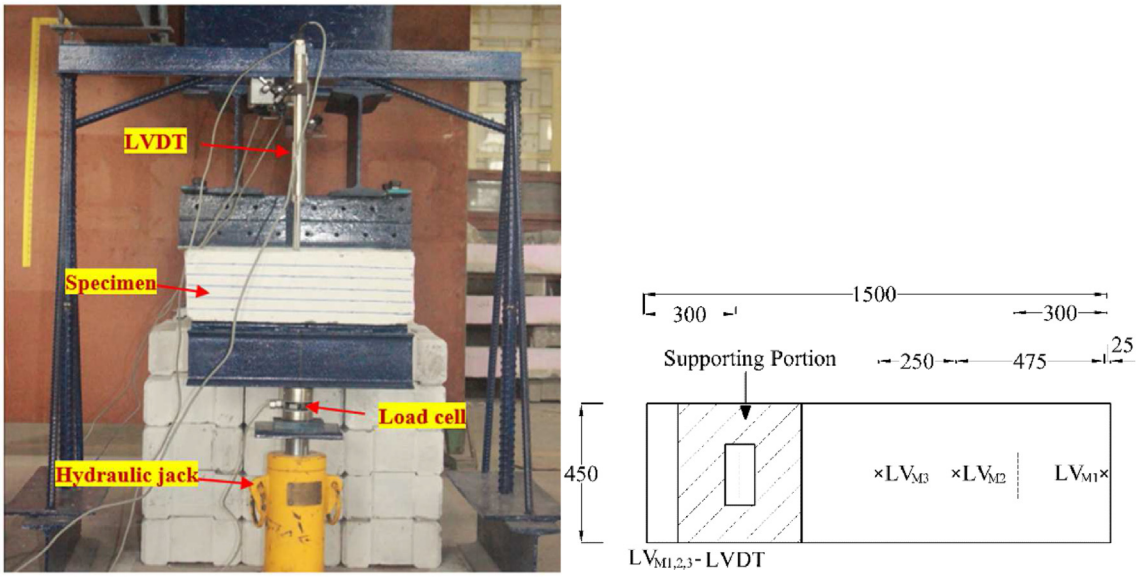

Fig. 5 – Picture showing the experimental setup for Mechanical loading.

using a 20 metric ton load cell. The readings were recorded using a data acquisition system.

3. Results and discussions

3.1. *Colour change*

In general, concrete specimens' colour change occurs at elevated temperatures, as shown in Figs. 6 and 7. The colour change can identify the temperature at which it was exposed, the area affected by that particular intensity and a rough estimation of the deterioration of mechanical properties of the reinforced concrete. The slow loss of water and subsequent drying of the cement paste, in addition to the changes that took place inside the aggregate, were responsible for the colour shift that occurred in heated concrete [50,51]. Assessment of damaged concrete due to an elevated temperature usually starts with a visual examination of spalling, cracking and colour change. However, it is vital to note that concrete not subject to colour change does not mean it was not damaged due to elevated temperature [52,53]. The colour

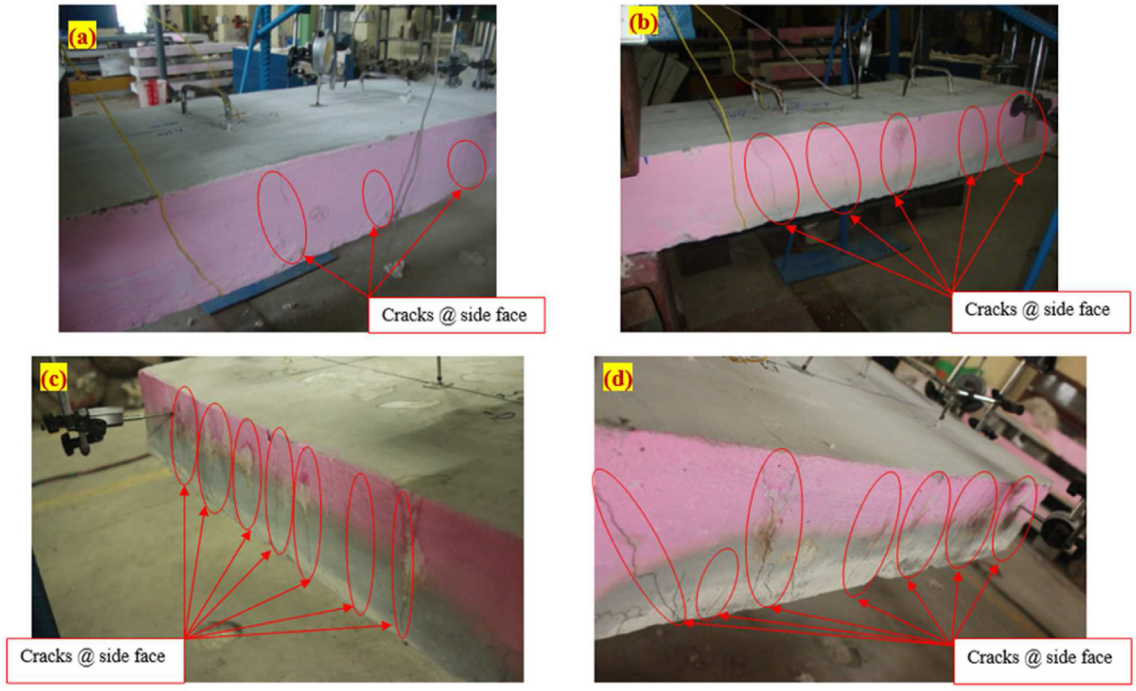

Fig. 6 – Colour change and cracks at a side face of 150 mm thick concrete slab – thermal loading (a) S1 (b) S2 (c) S3 (d) S4.

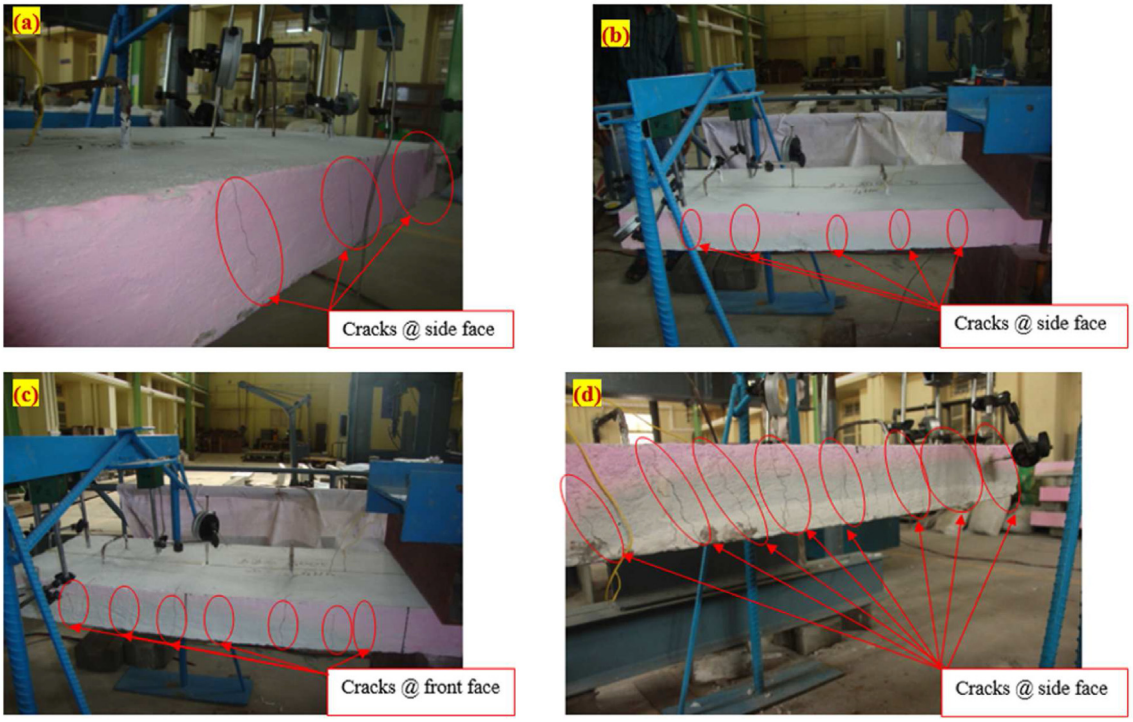

Fig. 7 – Colour change and crack at a side face of 100 mm thick concrete slab – thermal loading (a) S1 (b) S2 (c) S3 (d) S4.

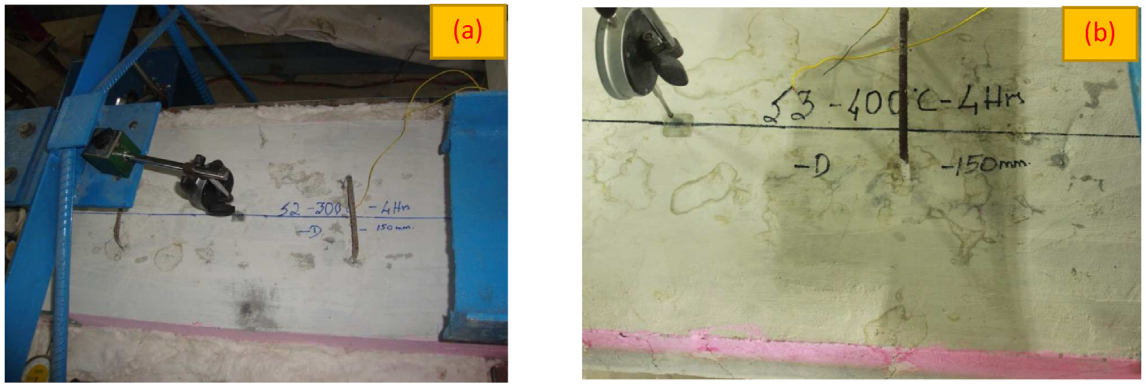

Fig. 8 – Oozing of water from tested specimens (a) water oozed out (b) water evaporated at tested specimens.

change was examined only on the external surface, especially at the sides. At 200 °C, there is no colour change along the slab's side surface. At 300 °C, grey colour to a depth of 40 mm from the soffit was observed. At 400 °C and 500 °C, two types of colour were noted along with the depth. The total colour change was observed for a depth of 65 mm and 78 mm for S3 and S4 slabs, respectively. The whitish-grey colour was observed from the exposed surface to 24 mm depth at 400 °C. At 500 °C, it was about 37 mm. The remaining depth of the slab was grey for S3 and S4 slabs.

3.2. *Moisture movement*

The excess water and chemically bound water started to ooze out at the sides and top surface of the slab when the temperature at the bottom surface of the concrete slab exceeded 200 °C, as shown in Fig. 8. It was found that moisture is forced away from the approaching heat front toward the top surface whenever the temperature within the slab continues to rise during the test. Similar findings were observed in the other studies [54,55]. The water tries to ooze out of cracks and pores formed due to heating, but in most cases, water oozing was around the lifting hooks on the top surface.

3.3. *Temperature distribution*

The furnace temperature was allowed to reach the bottom of the specimen, but the other surfaces were left accessible to the environment outside. The temperatures were measured at the top and bottom surfaces of the concrete slab at respective positions. The temperature variation at the top surface of the slab was very scanty, and the same was observed at the bottom

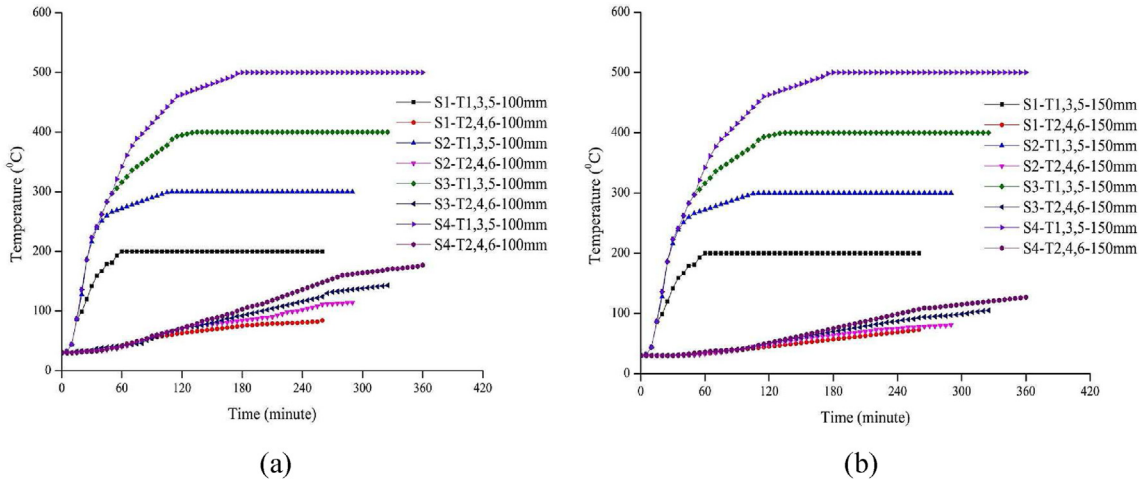

Fig. 9 – Time – average temperature relationship at top and bottom surface concrete slab a) 100 mm thick b) 150 mm thick.

surface, too; the variation in average temperature at the top surface and bottom surface of slabs with the function of times are as displayed in Fig. 9 (a) and (b). A similar pattern of distribution of temperature at the top surface and bottom surface of the slab was observed in previous studies [13,22,27,56].

Two different sets of failure criteria, both based on insulation, were proposed by a Eurocode (as a function of Separating) [55]. It is found that when any of the following criteria are met, it is considered that a slab has failed: (i) The non-exposed surface can only experience an increase in temperature of 140 °C on average, (ii) The temperature at the non-exposed surface of the slab should not be greater than are equal to 180 °C at any point on the non-exposed surface. Fig. 10 depicts insulation checks for 100 mm and 150 mm thick slabs. The S4 of the 100 mm slab exceeds the specified limit for insulation. S1, S2, and S3 of 100 mm thick slab and all the specimens of 150 mm thick slab show satisfactory performance over insulation criteria.

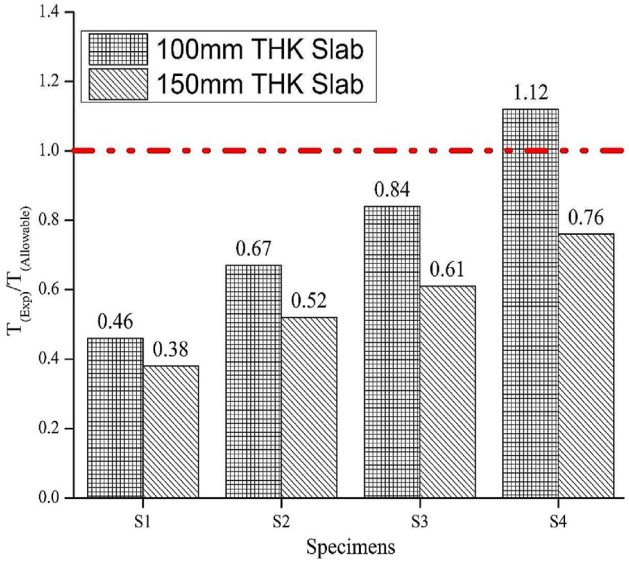

Fig. 10 – Insulation check for 100 mm and 150 mm thick concrete slab.

3.4. *Crack pattern and crack width*

The developments of cracks due to heating were visually observed during testing, at the sides of the slab and on the top surface. Measurements were also made of the crack's length and breadth. The crack width was measured using a digital crack width meter at 25 mm from the soffit during the last phases of heating. Table 2 and Table 3 demonstrate details of the height and number of visible cracks and crack width formed at the front face. It is observed that the crack width is larger at the bottom and narrows along with the depth, like an inverted "V".

Several cracks formed led to a longitudinal crack at the bottom of the slab, as shown in Figs. 11 and 12. However, detailed measurements of crack length at the bottom side were not possible due to the high temperature and the cracks started to close as the temperature source was removed. The closing of cracks was faster in case of quench cooling than in air-cooled conditions. Several cracks and cracks height were formed at the front face depending on the intensity of temperature. At the same time, the width of the crack depends on the intensity of temperature and the height from the exposed surface. After cooling to normal temperature, the crack width was less than 0.01 mm.

In the case of the side surface, many cracks formed at high temperatures. The formation of an inclined crack was also noticed at 500 °C. These cracks were developed and progressed towards the support like a shear crack, as shown in Figs. 6 and 7. The vertical cracks formed due to elevated temperature have a larger width at the exposed surface (soffit) of the slab. The spacing between cracks was reduced when the temperature increased and the spacing was noted between the cracks, which developed to a full depth. Table 4 and Table 5 provide detailed observations of cracks formed on the side surfaces of the concrete slab. Each crack was formed at different times during the period of exposure. It was observed that a crack was also formed between the cracks already formed due to heating. Sometimes the width of the exciting crack was reduced due to the formation of the new crack. So the formation of cracks can be described as non-proportional.

Table 2 – Details of the crack formed at the front face of 150 mm thick slab.

ID	Number of cracks	Maximum crack width in mm	Number of cracks					
			Height in mm					
			Lesser than 25	2–50	50–75	75–100	100–125	Greater than 125
S1-D/Q-200	3	0.03	2	1	–	–	–	–
S2-D/Q-300	5	0.08	1	1	1	1	1	–
S3-D/Q-400	7	0.20	4	1	–	1	1	–
S4-D/Q-500	10	0.29	4	2	1	1	–	2

Table 3 – Details of the crack formed at the front face of the 100 mm thick slab.

ID	Number of cracks	Maximum crack width in mm	Number of cracks			
			Height in mm			
			Lesser than 25	25–50	50–75	Greater than 75
S1-D/Q-200	3	0.03	2	1	–	–
S2-D/Q-300	4	0.09	2	2	1	1
S3-D/Q-400	7	0.21	3	2	1	1
S4-D/Q-500	10	0.28	4	2	3	1

Fig. 11 – Crack at top surface of 150 mm thick concrete slab - after quenching (a) S1 (b) S2 (c) S3.

Cracks were extensively formed on the top surface of the concrete slab when the concrete slab was exposed to elevated temperature, which was suddenly cooled by spraying water at the soffit of the slab for 30 min (as done during firefighting), as shown in Figs. 11 and 12. The cooling regimes played an important role in the formation of micro cracks in cement paste concrete due to sudden variation in temperature within the thickness of the slab under quench cooling. However, this state was not observed in the case of air-cooled specimens [57,58]. The specimens cooled by water or quenching were subjected to thermal shock, resulting in the formation of new cracks at the top surface of the concrete

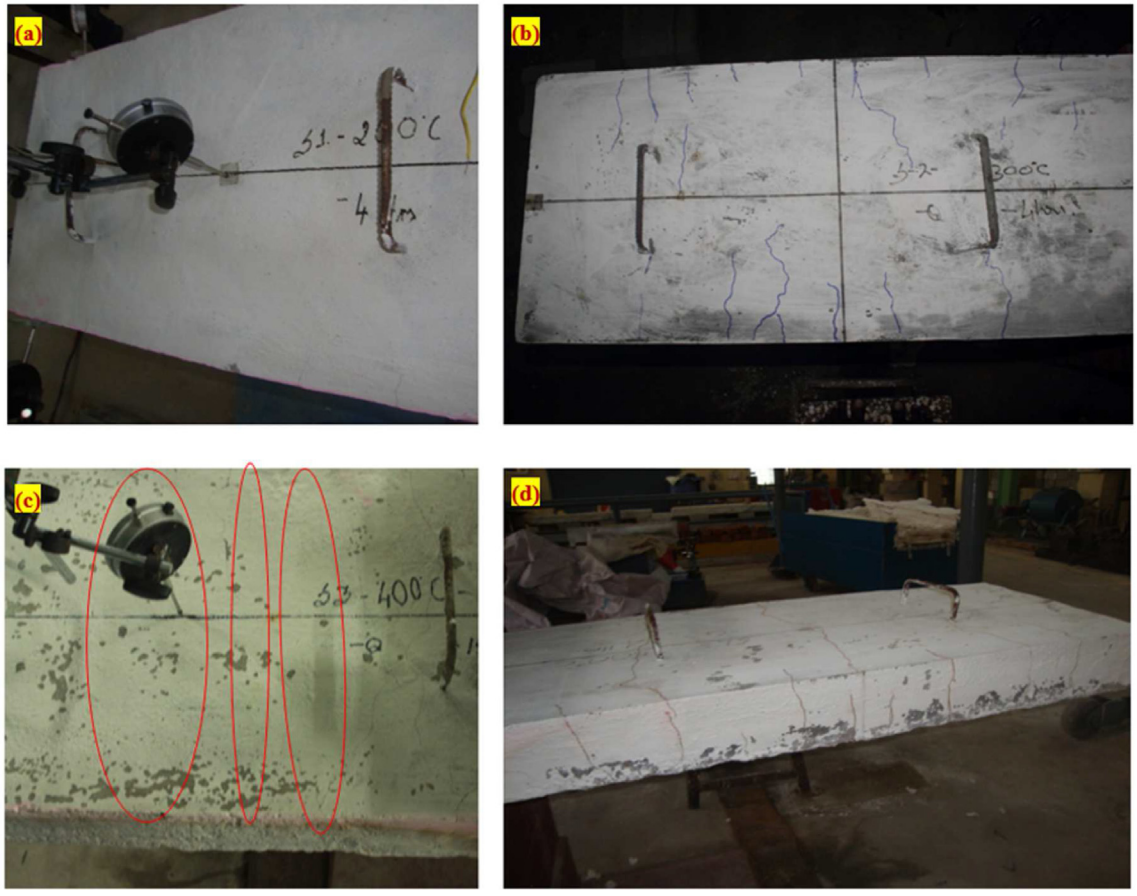

Fig. 12 – Crack at top surface of 100 mm thick concrete - after quenching (a) S1 (b) S2 (c) S3 (d) S4.

Table 4 – Details of crack at the side surface of 150 mm thick slab.

ID	Total number of cracks	Maximum Crack Width in mm	Number of cracks					
			Height in mm					
			Lesser than 25	25–50	50–75	75–100	100–125	Greater than 125
S1-D/Q-200	5	0.12	3	1	–	–	–	2
S2-D/Q-300	13	0.25	4	3	2	1	2	5
S3-D/Q-400	25	0.38	10	2	3	4	1	9
S4-D/Q-500	31	0.46	17	8	3	4	1	11

Table 5 – Details of crack at the side surface of 100 mm thick slab.

ID	Total number of cracks	Maximum Crack Width in mm	Number of cracks			
			Height in mm			
			Lesser than 25	25–50	50–75	Greater than 75
S1-D/Q-200	6	0.12	5	1	1	3
S2-D/Q-300	21	0.25	9	2	3	6
S3-D/Q-400	35	0.39	14	6	3	10
S4-D/Q-500	44	0.47	19	6	4	14

slab and internally. This effect is more pronounced in the slab subjected to temperatures 300 °C, 400 °C and 500 °C. The crack formation in 150 mm thick concrete slab was lesser than the 100 mm thick concrete slab in the case thermal loading. During the quenching process, cracks were formed at the top of a surface. Most of the cracks originated from the cracks, formed at the side surface and developed to a full depth during heating. These cracks were get interconnected by top surface cracks when subjected to quenching. The cracks and crack width formed under thermal loading were unsustain once the slabs were cooled down to atmospheric temperature.

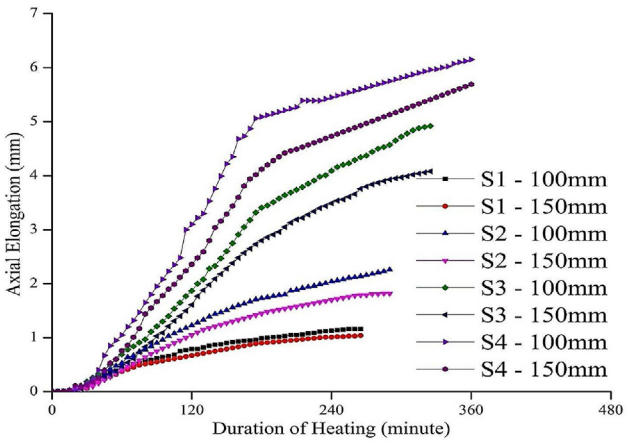

Fig. 13 – Axial elongation of 100 mm thick and 150 mm thick slab during the heating stage.

3.5. *Axial elongation*

Axial elongation is defined as the horizontal movement at a free end of the slab. The axial elongation were measured at half the thickness of the slab. Fig. 13 shows the axial deflection of 100 mm and 150 mm thick slabs plotted against the time recorded during the heating stages. The magnitude of deflection increases with an increase in exposure temperature. The horizontal deflection of the 100 mm thick slab at the end of the heating stage was 1.16 mm, 2.26 mm, 4.92 mm, and 6.15 mm for 200 °C–500 °C, respectively. In the case of a 150 mm thick slab, it was 1.04 mm, 1.82 mm, 4.08 mm and 5.69 mm. The residual elongation was always near zero for both types of cooling, but the deflection rate varies as per the condition considered in the test. The deflection rate was more significant in the quench-cooled specimen than in the air-cooled specimen. The pre-existing cracks in the structure due to heating results in geomentry non-linearity of structural elements before application of the Mecahnical Loading.

3.6. *Vertical deflection*

The slab started to deflect vertically away from the furnace once it was heated. Fig.. 14(a) and (b), clearly shows that the difference in vertical deflection magnitude depends upon exposure temperature, duration and thickness of slabs. The vertical deflection of a 100 mm slab subjected to 200 °C reaches 5.06 mm at 115 min and from this stage onwards, it was observed that the change in vertical deflection over time was insignificant. Similar observations were found for other exposed temperatures for all the specimens of 100 mm thick slab and 150 mm thick slab. The descending branch of vertical deflection measured for 30 min after desired exposure is shown in Fig. 14. This effect was due to the cooling condition used during testing. In the case of air-cooled specimens, a sudden variation during the initial period was observed and decreased gradually. However, for quench cooling, the drop was very sharp and measured deflection after 30 min cooling period was found to be 0.85 mm, 1.58 mm, 5.35 mm and 7.20 mm for S1-Q, S2-Q, S-Q and S4-Q of 100 mm thick slab respectively. The 150 mm thick slab was found to be 0.61 mm, 1.55 mm, 4.74 mm and 6.28 mm for S1-Q, S2-Q, S3-Q and S4-Q, respectively. The slab was deflected during the heating phase and reversing of the deflected shape during cooling conditions was observed by other researchers as well [13,22] The residual vertical deflection, which was measured after 8 h, was always near zero for both types of cooling. However, the deflection rate varies per the cooling condition considered in the test.

The flexural member failure criterion based on deflection limit state circumstances according to BS-476 [59] were as follows.

- When exposed to fire for any duration of time, the beam deflects more than L/20.
- The deflection rate surpasses the limit of $L^2/(9000 \times d)$
- Where d is the effective depth of the slab (mm) and L is the length of the slab in (mm).

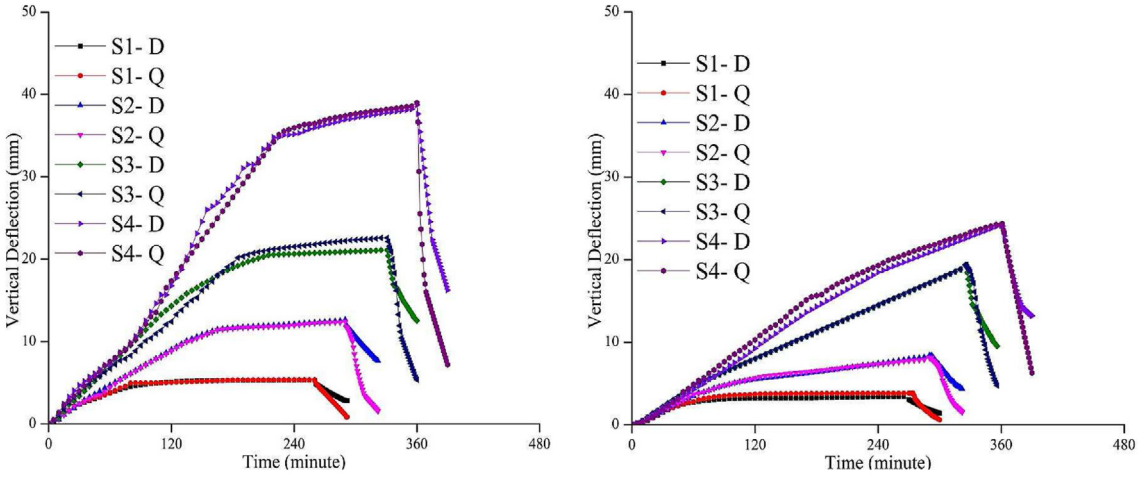

(a) 100 mm thick slab (b) 150 mm thick slab.

Fig. 14 – Vertical deflection of concrete slab for the various magnitude of temperature (a) 100 mm thick slab and (b) 150 mm thick slab.

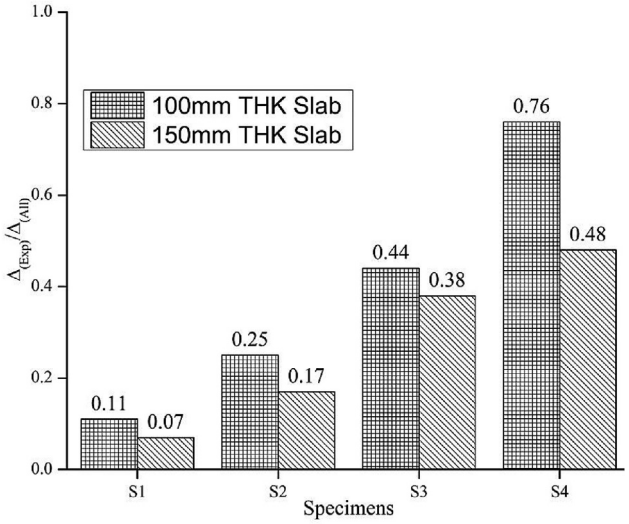

Fig. 15 – The ratio of ultimate deflection during the heating phase to BS-476 [37] recommends various thicknesses and high temperatures.

During the heating phase, the final deflection observed was compared to the allowed deflection parameters, as shown in Fig. 15. The ultimate deflections of the slabs were found to be within the limit specified. The deflection rate for different cooling conditions calculated during the cooling phase is shown in Fig.. 16 (a) and (b) have not exceeded the failure criteria specified (see Fig. 16).

4. Experimental – phase – II: mechanical loading

The assessment of residual strength and residual stiffness of fire-affected reinforced concrete elements is essential to decide whether they can be repaired or demolished. Fig. 17 (a) and (b) provide a detailed load versus deflection behavior of heat-affected 100 mm thick concrete specimens, which were air-cooled and quench-cooled, respectively. The graph indicates that the initial cracking load decreases for slabs exposed to higher temperature magnitude. Most slabs had a defined initial cracking load except for quench-cooled specimens exposed to 400 °C and 500 °C. This effect was due to the extensive cracks formed at the top of the slab resulting from quenching, as shown in Fig. 11 (c), 12 (c) and (d). The working load and ultimate load of slabs exposed to various temperatures matched the normal specimen, but the deflection for specific loads varies based on exposed temperature and cooling conditions.

Fig. 17 (a) and (b) indicate that the structure that deforms during heating and regains its original position during cooling has a definite loss in flexural stiffness of the specimens. The quantity of reduction in flexural stiffness depends on the thickness of the slab, exposed temperature and cooling conditions [10,11,60]. Compared to the thicknesses of the slab, the loss in flexural stiffness is less for the thicker slab for all the exposed temperatures, as shown in Fig. 18 (a) and (b). In the case of 200 °C, the reduction in flexural stiffness is very meager for both the thickness of the slab and for two different cooling conditions. The percentage reduction in flexural stiffness for 100 mm thick slab was 10.56%, 21.76% and 35.52% for 300 °C, 400 °C and 500 °C, respectively for air-cooled specimens. Similarly, for quench cooled conditions, the percentage loss in stiffness was 16.48%, 30.0% and 45.92% for 300 °C, 400 °C and 500 °C, respectively.

The study provides a clear idea about the reduction in the material strength and pre-existing cracks in the structural element due to thermal regimes resulting in further reduction in the moment of inertia, a function of the cross-sectional geometry. The above-specified reductions are the two essential properties of flexural Stiffness. The variation in loss percentage between air-cooled conditions and quench cooled is due to the effect of thermal shock that developed due to quenching which results in variation in thermal gradient between exposed surfaces and interior and unexposed surfaces [1008-. This effect increased with an increase in exposed

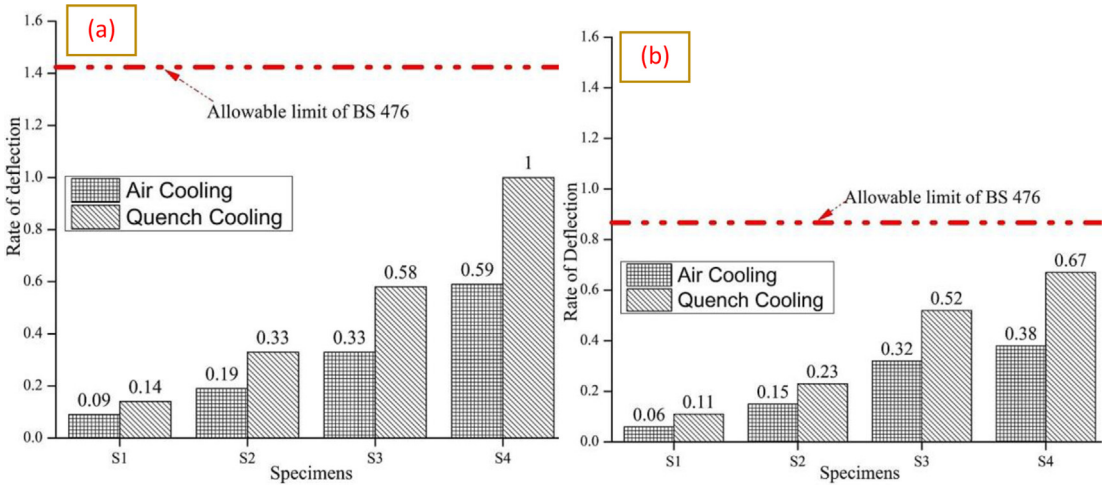

Fig. 16 – Comparison of deflection rate provided in BS-476 [37] and experimental results (a) 100 mm thick slab (b) 150 mm thick slab.

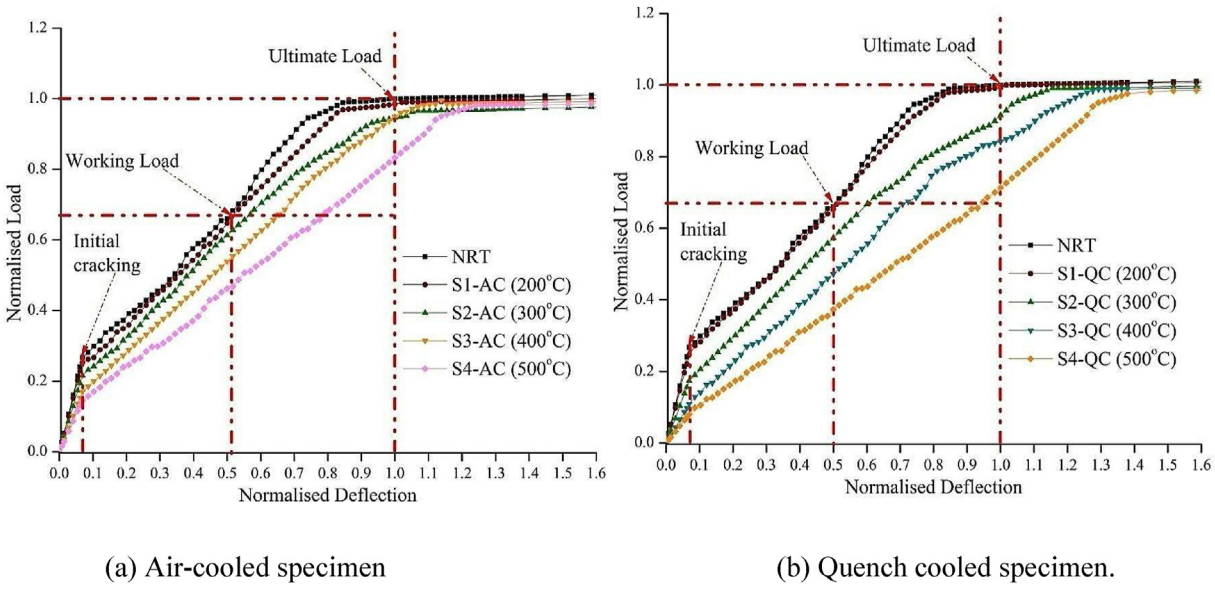

Fig. 17 – Normalized load versus displacement of 100 mm thick concrete slab (a) air-cooled specimen (b) quench-cooled specimen.

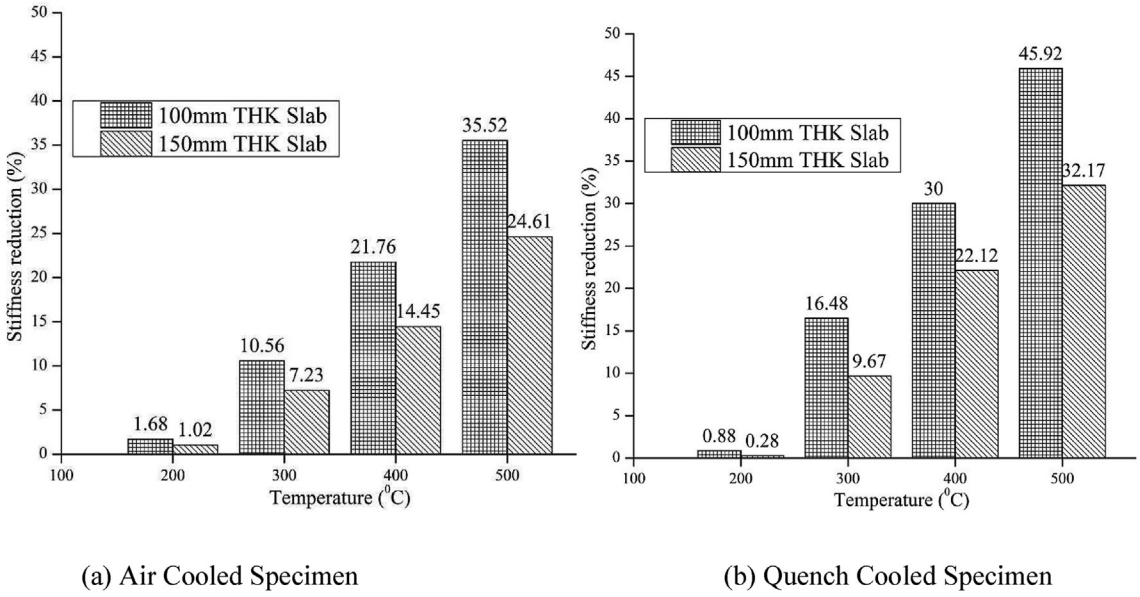

Fig. 18 – Percentage reduction in flexural stiffness after exposure to various temperatures a) air-cooled specimen b) quench-cooled specimen.

temperature and the loss percentage of flexural stiffness was maximum for slabs exposed to a temperature of 500 °C. The additional loss percentage of flexural stiffness in 100 mm thick slab for quench-cooled conditions were 5.92%, 8.24% and 10.36% compared to the air-cooled specimen for 300 °C, 400 °C and 500 °C, respectively. In the case of a 150 mm thick slab, the loss percentages were 7.23%, 14.45% and 24.61% for air-cooled specimens. In the quench-cooled specimen, the loss in stiffness was 9.67%, 22.12% and 32.17% for 300 °C, 400 °C and 500 °C, respectively. The additional percentage losses in stiffness for 100 mm thick slab compared to 150 mm thick slab were 3.3%, 7.26% and 10.91% for 300 °C, 400 °C and 500 °C, respectively, for the air-cooled specimen. In the case of quench-cooled specimens, it was 6.81%, 7.88% and 13.75% for 300 °C, 400 °C and 500 °C, respectively. The loss in stiffness of the quench-cooled members was more than that of the air-cooled specimens due to thermal shock action and coarsening of pores [40–42,44].

The cracking and crushing of concrete at the fixed end during the mechanical loading are shown in Fig. 19 (a)–(d). The initial cracks developed at the maximum moment zone, and as the test continued, some cracks that were formed already due to heating and cooling between supports to half the length of the member widened [10,12]. Cracks developed to the full depth of the slab, as shown in Fig. 19 (a), were found in all the slabs. The crushing failure of concrete was witnessed

a) Cracking of Specimen in the tension zone under mechanical loading

b) Initiation of Compression Failure in the Concrete Specimen under Mechanical Loading

Fig. 19 – Failure pattern of thermally exposed concrete Slabs under mechanical loading.

in S3-(D&Q)-100, S4-(D&Q)-100, S3-Q-150 and S4-150-(D&Q). In S2-Q-100 and S3-D-150, out of three slabs, one slab initiated the crushing failure of concrete.

5. Conclusions

The concrete compressive strength and stiffness were negatively impacted by cooling regimes such as air and quench cooling conditions. However, it also depends on the temperature intensity and exposure duration. The residual strength of concrete specimens cooled with water for a short time exhibited a dramatic fluctuation when the temperature was more than 200 °C. The need is to assess the level of damage based on the specimen's load-bearing capacity and flexural stiffness. The paper aims to bring out a realistic view of slab elements during and after being exposed to elevated temperatures. The research focused on the temperature at the non-exposed surface, crack formation, and crack width during the heating and cooling stages, during the mechanical loading stage mode of failure, the behavior of the cantilever slab, and variation in residual strength and flexural stiffness. Based on the detailed investigation, the key findings are summarized as follows.

- The visual observation may be illusory as all the observations are carried out on the heated and cooled structure. Sometimes, the physical and chemical changes that occur during heating are not visible once the heat in the structural element is reduced to atmospheric conditions. The colour change provided information about the temperature distribution across the depth of the slab. If the colour change did not occur, it does not mean it was not damaged due to elevated temperature.
- Since the slab is a vertical separation element, insulation criteria are critical. The specimen fails in this criteria, but other slabs show good insulation resistance.
- The crack depth, number of cracks, and width formed depend on the magnitude and temperature to which the slab was exposed. The formation of cracks during the heating stage does not follow any sequence or theory; it is random and highly non-proportional. The cracks formed during the heating stage are closer when the slab heat is reduced to the atmospheric level.
- The deflection ratio increased from 0.11 to 0.76 for a 100 mm thick slab. In the case of a 150 mm thick slab, the deflection ratio varies from 0.07 to 0.48. The ratio was minimum for temperature (200 °C) and maximum for (500 °C). The ratio of the rate of deflection was found to increase from 0.09 to 0.59 for a 100 mm thick slab under air cooling from 200 °C to 500 °C. Quench cooling varies from 0.14 to 1.00 from 200 °C to 500 °C.
- It is revealed that in a 150 mm thick slab, the ratio of the rate of deflection varies from 0.06 to 0.38 for air-cooled

specimens. The ratio varies from 0.11 to 0.67 for quench-cooled conditions. Based on the cooling condition for two different thicknesses, the quench-cooled specimen has more magnitude than the air-cooled specimen. The maximum range was observed in the 100 mm thick slab for all the temperatures.

- The residual flexural stiffness of the specimens and the various failure criteria varied significantly depending on the cooling process used. Due to the heating and cooling methods, the material's flexural stiffness is reduced. In a 100 mm thick slab, the flexural stiffness reduction varies from 1.68% to 35.52% for a temperature range of 200 °C–500 °C under air-cooled conditions.
- In the case of quench cooled, it is found that it was varied between 0.88% and 45.92% for a temperature range of 200 °C–500 °C. For the slab element with 150 mm thick, the percentage reduction in flexural stiffness for air-cooled specimens was 1.02%–24.61% for a temperature range of 200 °C–500 °C. Similarly, for the quench-cooled case, the reduction in stiffness varies from 0.28% to 32.17% for a temperature range of 200 °C–500 °C.
- The quenching effect was found to have a very slight negative effect at 200 °C for both slab thicknesses. The quenching effect resulted in more destruction in the case of flexural stiffness of the element than air-cooled for temperatures above 200 °C. Flexural stiffness reduction also depends on the exposed temperature and slabs' thickness. Slabs with less thickness resulted in more reduction in flexural stiffness.
- The failure criteria vary for different specimens and depend on the exposed temperature and cooling condition. It generally exhibited that the type of final failure of the specimens is a crushing failure of concrete.
- Drastic variations in stiffness between quench-cooled and air-cooled specimens were observed for specimens exposed at 300 °C, 400 °C and 500 °C for the 100 mm and 150 mm thick slab. The drastic variation was due to the effect of thermal shock that developed because of quenching, leading to variation in thermal gradient between exposed surface, interior and unexposed surface.
- The firefighters should spray the water from outside rather than enter the fire-exposed building. It is also better to provide some time gap to enter the building after the fire.
- It is also revealed that the slab element exposed to a temperature of 300 °C and 400 °C can be repaired and, at 500 °C to be demolished.

Future developments

- The present study only studied the experimental evaluation of the strength degradation under various heating and cooling regimes. Further development of a numerical model is essential to predict the mechanical behavior of structural elements under various cooling phases.
- Extensive laboratory testing is required to predict the materials properties and behavior under the cooling regimes. An analytical approach can be proposed to stimulate the mechanical behavior of materials under cooling regimes.

Declaration of competing interest

The authors declare that they have no known competing financial interests or personal relationships that could have appeared to influence the work reported in this paper.

Acknowledgments

The authors gratefully acknowledge that: “This study is supported via funding from Prince Sattam bin Abdulaziz University project number (PSAU/2023/R/1444)”.

REFERENCES

[1] Bratina S, Saje M, Planinc I. The effects of different strain contributions on the response of RC beams in fire. Eng Struct 2007;29:418–30. https://doi.org/10.1016/j.engstruct.2006.05.008.

[2] Lee YH, Chua N, Amran M, Lee YY, Kueh AH, Fediuk R, Vatin N, Vasilev Y. Thermal performance of structural lightweight concrete composites for potential energy saving, vols. 1–15; 2021.

[3] George C, Lee SBM, Huang Chao, Bastam N, Fard A. Study of U.S., bridge failures (1980-2012). University at Buffalo, State University of New York; 2013. p. 148.

[4] Daneshvar K, Moradi MJ, Khaleghi M, Rezaei M, Farhangi V, Hajiloo H. Effects of impact loads on heated-and-cooled reinforced concrete slabs. J Build Eng 2022:105328. https://doi.org/10.1016/j.jobe.2022.105328.

[5] Amran M, Huang SS, Debbarma S, Rashid RSM. Fire resistance of geopolymer concrete: a critical review. Construct Build Mater 2022:324.

[6] Amran M, Huang S-S, Onaizi AM, Murali G, Abdelgader HS. Fire spalling behavior of high-strength concrete: a critical review. Construct Build Mater 2022;341:127902. https://doi.org/10.1016/j.conbuildmat.2022.127902.

[7] Amran M, Fediuk R, Klyuev S, Qader DN. Sustainable development of basalt fiber-reinforced high-strength eco-friendly concrete with a modified composite binder. Case Stud Constr Mater 2022;17:e01550. https://doi.org/10.1016/j.cscm.2022.e01550.

[8] Weerasinghe P, Nguyen K, Mendis P, Guerrieri M. Large-scale experiment on the behaviour of concrete flat slabs subjected to standard fire. J Build Eng 2020:30. https://doi.org/10.1016/j.jobe.2020.101255.

[9] Drury MM, Kordosky AN, Quiel SE. Robustness of a partially restrained, partially composite steel floor beam to natural fire exposure: novel validation and parametric analysis. J Build Eng 2021;44. https://doi.org/10.1016/j.jobe.2021.102533.

[10] Wang Y, Ren Z, Huang Z, Gao W, Zhong B, Bu Y, Huang Y, Zhang Y, Yuan G, Ma S. Experimental and numerical studies of six small-scale continuous concrete slabs subjected to travelling fires. Eng Struct 2021:236. https://doi.org/10.1016/j.engstruct.2021.112069.

[11] Wang Y, Wu J, Huang Z, Jiang J, Yuan G, Zhang Y, Jiang Y, Chen Z, Zhou M. Experimental studies on continuous reinforced concrete slabs under single and multi-compartment fires with cooling phase. Fire Saf J 2020;111. https://doi.org/10.1016/j.firesaf.2019.102915.

[12] Wang Y, Yuan G, Huang Z, Lyv J, Li ZQ, Wang T. Yan Experimental study on the fire behaviour of reinforced concrete slabs under combined uni-axial in-plane and out-

of-plane loads. Eng Struct 2016;128:316–32. https://doi.org/10.1016/j.engstruct.2016.09.054.
[13] Wang Y, Bisby LA, Wang T yan, Yuan G, Baharudin E. Fire behaviour of reinforced concrete slabs under combined biaxial in-plane and out-of-plane loads. Fire Saf J 2018;96:27–45. https://doi.org/10.1016/j.firesaf.2017.12.004.
[14] Bailey CG, Toh WS. Small-scale concrete slab tests at ambient and elevated temperatures. Eng Struct 2007;29:2775–91. https://doi.org/10.1016/j.engstruct.2007.01.023.
[15] Bailey CG, Toh WS. Behaviour of concrete floor slabs at ambient and elevated temperatures. Fire Saf J 2007;42:425–36. https://doi.org/10.1016/j.firesaf.2006.11.009.
[16] Cao V Van, Vo HB, Dinh LH, Doan D Van. Experimental behavior of fire-exposed reinforced concrete slabs without and with FRP retrofitting. J Build Eng 2022:51. https://doi.org/10.1016/j.jobe.2022.104315.
[17] Saleheen Z, Krishnamoorthy RR, Nadjai A. A review on behavior, material properties and finite element simulation of concrete tunnel linings under fire. Tunn Undergr Space Technol 2022:126. https://doi.org/10.1016/j.tust.2022.104534.
[18] Andrushia AD, Anand N, Neebha TM, Naser MZ, Lubloy E. Autonomous detection of concrete damage under fire conditions. Autom ConStruct 2022;140:104364. https://doi.org/10.1016/j.autcon.2022.104364.
[19] Kontoleon KJ, Georgiadis-Filikas K, Tsikaloudaki KG, Theodosiou TG, Giarma CS, Papanicolaou CG, Triantafillou TC, Asimakopoulou EK. Vulnerability assessment of an innovative precast concrete sandwich panel subjected to the ISO 834 fire. J Build Eng 2022:52. https://doi.org/10.1016/j.jobe.2022.104479.
[20] Mubarak M, Muhammad Rashid RS, Amran M, Fediuk R, Vatin N, Klyuev S. Mechanical properties of high-performance hybrid fibre-reinforced concrete at elevated temperatures. Sustainability 2021;13:13392.
[21] Hua N, Elhami Khorasani N, Tessari A, Ranade R. Experimental study of fire damage to reinforced concrete tunnel slabs. Fire Saf J 2022;127. https://doi.org/10.1016/j.firesaf.2021.103504.
[22] Wang Y, Duan Y, Ma S, Huang Z, Zhang Y, Wu J, Yuan G, Zhou M, Zhang G. Behaviour of continuous reinforced concrete floor slabs subjected to different compartment fires. Eng Struct 2019;197. https://doi.org/10.1016/j.engstruct.2019.109445.
[23] Wang Y, Chen Z, Jiang Y, Huang Z, Zhang Y, Huang Y, Li L, Wu J, Guo W. Residual properties of three-span continuous reinforced concrete slabs subjected to different compartment fires. Eng Struct 2020:208. https://doi.org/10.1016/j.engstruct.2020.110352.
[24] Wang Y, Jiang Y, Huang Z, Li L, Huang Y, Zhang Y, Zhang G, Zhang X, Duan Y. Post-fire behaviour of continuous reinforced concrete slabs under different fire conditions. Eng Struct 2021:226. https://doi.org/10.1016/j.engstruct.2020.111342.
[25] Yu JT. Thesis. In: Experimental and theoretical research on damage assessment of reinforced concrete member after fire. Shanghai: Tongji University; 2007.
[26] Bolina FL, Tutikian B, Rodrigues JPC. Experimental analysis on the structural continuity effect in steel decking concrete slabs subjected to fire. Eng Struct 2021:240. https://doi.org/10.1016/j.engstruct.2021.112299.
[27] Wang Y, Wang G, Huang Z, Huang Y, Wang B, Gu A, Zhang C, Jiang Y, Zhang X. Experimental studies and theoretical analysis of the residual properties of three-span small-scale continuous concrete slabs after a fire. Fire Saf J 2021;126. https://doi.org/10.1016/j.firesaf.2021.103481.
[28] Usmani AS, Cameron NJK. Limit capacity of laterally restrained reinforced concrete floor slabs in fire. Cement Concr Compos 2004;26:127–40. https://doi.org/10.1016/S0958-9465(03)00090-8.
[29] Omer E, Izzuddin BA, Elghazouli AY. Failure of unrestrained lightly reinforced concrete slabs under fire, Part I: analytical models. Eng Struct 2010;32:2631–46. https://doi.org/10.1016/j.engstruct.2010.04.039.
[30] Lim L, Wade C. Experimental fire tests of two-way concrete slabs - fire engineering research report 02/12. 2002. p. 1–96.
[31] Zhang D, Dong Y. Theoretical model for limit load-carrying capacity of one-way concrete slabs at large displacements. Advances in Information Sciences and Service Sciences 2012;4:235–43. https://doi.org/10.4156/AISS.vol4.issue10.28.
[32] Mugahed Amran YH, El-Zeadani M, Raizal Saifulnaz MR, Alyousef R, Alabduljabbar H, Alrshoudi F, Alaskar A. RC beam strengthening using hinge and anchorage approach. Results in Materials 2020;5. https://doi.org/10.1016/j.rinma.2019.100047.
[33] Guo S, Bailey CG. Experimental behaviour of composite slabs during the heating and cooling fire stages. Eng Struct 2011;33:563–71. https://doi.org/10.1016/j.engstruct.2010.11.014.
[34] Lee YH, Amran M, Lee YY, Kueh ABH, Kiew SF, Fediuk R, Vatin N, Vasilev Y. Thermal behavior and energy efficiency of modified concretes in the tropical climate: a systemic review. Sustainability 2021;13.
[35] Huang Z. The behaviour of reinforced concrete slabs in fire. Fire Saf J 2010;45:271–82. https://doi.org/10.1016/j.firesaf.2010.05.001.
[36] Colombo M, Martinelli P, Arano A, Øverli JA, Hendriks MAN, Kanstad T, di Prisco M. Experimental investigation on the structural response of RC slabs subjected to combined fire and blast. Structures 2021;31:1017–30. https://doi.org/10.1016/j.istruc.2021.02.029.
[37] Al-Ameri RA, Abid SR, Murali G, Ali SH, Özakça M, Vatin NI. Residual impact performance of ECC subjected to sub-high temperatures. Materials 2022;15. https://doi.org/10.3390/ma15020454.
[38] Cooke GME. Deflections of concrete floor slabs exposed to standardised fires and some implications for design. Struct Eng 2001;79:26–34.
[39] Poon C-S, Azhar S, Anson M, Wong Y-L. Strength and durability recovery of fire-damaged concrete after post-fire-curing. Cement Concr Res 2001;31:1307–18.
[40] Peng GF, Bian SH, Guo ZQ, Zhao J, Peng XL, Jiang YC. Effect of thermal shock due to rapid cooling on residual mechanical properties of fiber concrete exposed to high temperatures. Construct Build Mater 2008;22:948–55. https://doi.org/10.1016/j.conbuildmat.2006.12.002.
[41] Bingöl AF, Gül R. Effect of elevated temperatures and cooling regimes on normal strength concrete. Fire Mater 2009;33:79–88. https://doi.org/10.1002/fam.987.
[42] Shen J, Xu Q. Effect of elevated temperatures on compressive strength of concrete. Construct Build Mater 2019;229. https://doi.org/10.1016/j.conbuildmat.2019.116846.
[43] Tung TM, Emmanuel BO, Duc-Hien L. Experimental investigation of the performance of ground granulated blast furnace slag blended recycled aggregate concrete exposed to elevated temperatures. Cleaner Waste Systems 2022;2023(4):100069.
[44] Gallucci E, Zhang X, Scrivener KL. Effect of temperature on the microstructure of calcium silicate hydrate (C-S-H). Cement Concr Res 2013;53:185–95. https://doi.org/10.1016/j.cemconres.2013.06.008.
[45] IS 10262 : 2009 Guidelines for concrete mix design proportioning. New Delhi, India: Bureau of Indian Standards; 2009.
[46] Haridharan MK, Natarajan C, Chen SE. Evaluation of residual strength and durability aspect of concrete cube exposed to

elevated temperature. Journal of Sustainable Cement-Based Materials 2017;6:231–53. https://doi.org/10.1080/21650373.2016.1230898.
[47] IS:8112. Specification for 43 Grade ordinary Portland cement. Bureau of Indian standards. New Delhi: Bureau of Indian Standards; 1989. p. 17. India.
[48] ASTM C618-17a *Standard specification for* Coal fly ash and raw or calcined natural pozzolan for use in concrete. 2017.
[49] IS 3812-1 (2013): Specification for pulverized fuel ash, Part 1: for use as pozzolana in cement, cement mortar and concrete. Bureau of Indian standards; 2013.
[50] Colombo M, Felicetti R. New NDT techniques for the assessment of fire-damaged concrete structures. Fire Saf J 2007;42:461–72. https://doi.org/10.1016/j.firesaf.2006.09.002.
[51] Zeyad AM, Johari MAM, Alharbi YR, Abadel AA, Amran YHM, Tayeh BA, Abutaleb A. Influence of steam curing regimes on the properties of ultrafine POFA-based high-strength green concrete. J Build Eng 2021:38. https://doi.org/10.1016/j.jobe.2021.102204.
[52] Annerel E, Taerwe L. Revealing the temperature history in concrete after fire exposure by microscopic analysis. Cement Concr Res 2009;39:1239–49. https://doi.org/10.1016/j.cemconres.2009.08.017.
[53] Hager I. Colour change in heated concrete. Fire Technol 2014;50:945–58. https://doi.org/10.1007/s10694-012-0320-7.
[54] Ali F, Nadjai A, Abu-Tair A. Explosive spalling of normal strength concrete slabs subjected to severe fire. Materials and Structures/Materiaux et Constructions 2011;44:943–56. https://doi.org/10.1617/s11527-010-9678-5.
[55] En NP. Eurocode 2 - design of concrete structures Part 1-2: general rules Structural fire design. 2010. p. 109.
[56] Rosa IC, Santos P, Firmo JP, Correia JR. Fire behaviour of concrete slab strips reinforced with sand-coated GFRP bars. Compos Struct 2020;244. https://doi.org/10.1016/j.compstruct.2020.112270.
[57] Luo X, Sun W, Chan SYN. Effect of heating and cooling regimes on residual strength and microstructure of normal strength and high-performance concrete. Cement Concr Res 2000;30:379–83. https://doi.org/10.1016/S0008-8846(99)00264-1.
[58] Nassif AY. Postfiring stress-strain hysteresis of concrete subjected to various heating and cooling regimes. Fire Mater 2002;26:103–9. https://doi.org/10.1002/fam.785.
[59] BSI BS 476-3. Fire tests on building materials and structures. Classification and method of test for external fire exposure to roofs, vol. 16; 2004. 2004.
[60] Shachar YM, Dancygier AN. Assessment of reinforced concrete slabs post-fire performance. Fire Saf J 2020;111. https://doi.org/10.1016/j.firesaf.2019.102932.